Three-component Fermi gas with SU(3) symmetry: BCS-BEC crossover in three and two dimensions

L. Salasnich

Dipartimento di Fisica "Galileo Galilei" and CNISM,

Università di Padova,

Via Marzolo 8, 35122 Padova, Italy

E-mail: luca.salasnich@unipd.it

Abstract

We analyze the crossover from the Bardeen-Cooper-Schrieffer (BCS) state of weakly bound Fermi pairs to the Bose-Einstein condensate (BEC) of molecular dimers for a Fermi gas made of neutral atoms in three hyperfine states with a SU(3) invariant attractive interaction. By solving the extended BCS equations for the total number of particles and the pairing gap, we calculate at zero temperature the pairing gap, the population imbalance, the condensate fraction and the first sound velocity of the uniform system as a function of the interaction strength in both three and two dimensions. Contrary to the three-dimensional case, in two dimensions the condensate fraction approaches the value 1 only for an extremely large interaction strength and, moreover, the sound velocity gives a clear signature of the disappearance of one of the three hyperfine components.

I. INTRODUCTION

In the last years degenerate ultracold gases made of bosonic or fermionic atoms have been the subject of intense experimental and theoretical research [1, 2]. Among the several hot topics recently investigated, let us remind the expansion of a Fermi superfluid in the crossover from the Bardeen-Cooper-Schrieffer (BCS) state of weakly bound Fermi pairs to the Bose-Einstein condensate (BEC) of molecular dimers [3, 4]; the surface effects in the unitary Fermi gas [5]; the localization of matter waves in optical lattices [6]; the transition to quantum turbolence in finite-size superfluids [7, 8].

Very recently degenerate three-component gases have been experimentally realized using the three lowest hyperfine states of ^{6}Li [9, 10]. At high magnetic fields the scattering lengths of this three-component system are very close each other and the system is approximately SU(3) invariant. Moreover, it has been theoretically predicted that good $SU(N)$ invariance (with $N \leq 10$) can be reached with ultracold alkaline-earth atoms (e.g. with ^{87}Sr atoms) [11–13]. In the past various authors [14–17] have considered the BCS regime of a fermionic gas with SU(3) symmetry. In the last years He, Jin and Zhang [18] and Ozawa and Baym [19] have investigated the full BCS-BEC crossover [20–24] of this system at zero and finite temperature in three-dimensional space. Recently we have calculated the condensate fraction and the population imbalance for this three-component quantum gas both in the three-dimensional case and in the two-dimensional one [25]. In this paper we review the extended BEC theory [21–23] for an atomic gas with three-component fermions at zero temperature [18, 19, 25] but without invoking functional integration. We obtain the chemical potential, the energy gap, the number densities and the condensate fraction as a function of the adimensional interaction strength. Finally, we calculate also the first sound velocity of the system both in three and two dimensions. In two dimensions we find that the sound velocity shows a kink at the critical strength (scaled binding energy) where one of the three hyperfine components goes to zero.

The Lagrangian density of a dilute and ultracold three-component uniform Fermi gas of neutral atoms is given by

$$\hat{\mathcal{L}} = \sum_{\alpha=R,G,B} \hat{\psi}_\alpha^+ \left(i\hbar \frac{\partial}{\partial t} + \frac{\hbar^2}{2m} \nabla^2 + \mu \right) \hat{\psi}_\alpha - g \left(\hat{\psi}_R^+ \hat{\psi}_G^+ \hat{\psi}_G \hat{\psi}_R + \hat{\psi}_R^+ \hat{\psi}_B^+ \hat{\psi}_B \hat{\psi}_R + \hat{\psi}_G^+ \hat{\psi}_B^+ \hat{\psi}_B \hat{\psi}_G \right) ,$$

(1)

where $\hat{\psi}_\alpha(\mathbf{r}, t)$ is the field operator that destroys a fermion of component α in the position

2

r at time t, while $\hat{\psi}_\alpha^+(\mathbf{r})$ creates a fermion of component α in **r** at time t. To mimic QCD the three components are thought as three colors: red (R), green (G) and blue (B). The attractive inter-atomic interaction is described by a contact pseudo-potential of strength g ($g < 0$). The average total number of fermions is given by

$$N = \sum_{\alpha=R,G,B} \int \langle \hat{\psi}_\alpha^+(\mathbf{r},t)\hat{\psi}_\alpha(\mathbf{r},t) \rangle \, d^3\mathbf{r} , \tag{2}$$

where $\langle \cdots \rangle$ is the ground-state average. Note that N is fixed by the chemical potential μ which appears in Eq. (1). As stressed in Refs. [18, 19], by fixing only the total chemical potential μ (or equivalently only the total number of atoms N) the Lagrangian (1) is invariant under global SU(3) rotations of the species.

II. EXTENDED BCS EQUATIONS

At zero temperature the attractive interaction leads to pairing of fermions which breaks the SU(3) symmetry but only two colors are paired and one is left unpaired [18, 19, 25]. We assume, without loss of generality [18, 19, 25], that the red and green particles are paired and the blue are not paired. The interacting terms can be then treated within the minimal mean-field BCS approximation, i.e. neglecting the Hartree terms while the pairing gap

$$\Delta = g \, \langle \hat{\psi}_G(\mathbf{r},t)\hat{\psi}_R(\mathbf{r},t) \rangle \tag{3}$$

between red and green fermions is the key quantity. In this way the mean-field Lagrangian density becomes

$$\hat{\mathcal{L}}_{mf} = \sum_{\alpha=R,G,B} \hat{\psi}_\alpha^+ \left(i\hbar\frac{\partial}{\partial t} + \frac{\hbar^2}{2m}\nabla^2 + \mu \right) \hat{\psi}_\alpha + \Delta \, \hat{\psi}_G \hat{\psi}_R + \Delta \, \hat{\psi}_G^+ \hat{\psi}_R^+ , \tag{4}$$

under the simplifying condition that the pairing gap is real, i.e. $\Delta^* = \Delta$. It is then straightforward to write down the Heisenberg equations of motion of the field operators:

$$i\hbar\frac{\partial}{\partial t}\hat{\psi}_R = \left(-\frac{\hbar^2}{2m}\nabla^2 - \mu \right) \hat{\psi}_R + \Delta \, \hat{\psi}_G^+ , \tag{5}$$

$$i\hbar\frac{\partial}{\partial t}\hat{\psi}_G = \left(-\frac{\hbar^2}{2m}\nabla^2 - \mu \right) \hat{\psi}_G + \Delta \, \hat{\psi}_R^+ , \tag{6}$$

$$i\hbar\frac{\partial}{\partial t}\hat{\psi}_B = \left(-\frac{\hbar^2}{2m}\nabla^2 - \mu \right) \hat{\psi}_B , \tag{7}$$

3

which are coupled by the presence of the same chemical potential μ in the three equations. We now use the Bogoliubov-Valatin representation of the field operator $\hat{\psi}_\alpha(\mathbf{r}, t)$ in terms of the anticommuting quasi-particle Bogoliubov operators $\hat{b}_{\mathbf{k}\alpha}$:

$$\hat{\psi}_R(\mathbf{r}, t) = \sum_\mathbf{k} \left(u_k e^{i(\mathbf{k}\cdot\mathbf{r}-\omega_k t)} \hat{b}_{\mathbf{k}R} - v_k e^{-i(\mathbf{k}\cdot\mathbf{r}-\omega_k t)} \hat{b}_{\mathbf{k}G}^+ \right) , \tag{8}$$

$$\hat{\psi}_G(\mathbf{r}, t) = \sum_\mathbf{k} \left(u_k e^{i(\mathbf{k}\cdot\mathbf{r}-\omega_k t)} \hat{b}_{\mathbf{k}G} + v_k e^{-i(\mathbf{k}\cdot\mathbf{r}-\omega_k t)} \hat{b}_{\mathbf{k}R}^+ \right) , \tag{9}$$

$$\hat{\psi}_B(\mathbf{r}, t) = \sum_\mathbf{k} e^{i(\mathbf{k}\cdot\mathbf{r}-\Omega_k t)} \hat{b}_{\mathbf{k}B} , \tag{10}$$

where u_k and v_k are such that $u_k^2 + v_k^2 = 1$. After inserting these expressions into the Heisenberg equations of motion of the field operators we get

$$\xi_k = \hbar\Omega_k = \frac{\hbar^2 k^2}{2m} - \mu , \tag{11}$$

$$E_k = \hbar\omega_k = \sqrt{\xi_k^2 + \Delta^2} , \tag{12}$$

and also

$$u_k^2 = \frac{1}{2}\left(1 + \frac{\xi_k}{E_k}\right) , \qquad v_k^2 = \frac{1}{2}\left(1 - \frac{\xi_k}{E_k}\right) . \tag{13}$$

By imposing the following ground-state averages

$$\langle \hat{b}_{\mathbf{k}B}^+ \hat{b}_{\mathbf{k'}B} \rangle = \Theta(-\xi_k)\,\delta_{\mathbf{k},\mathbf{k'}} , \qquad \langle \hat{b}_{\mathbf{k}R}^+ \hat{b}_{\mathbf{k}R} \rangle = \langle \hat{b}_{\mathbf{k}G}^+ \hat{b}_{\mathbf{k}G} \rangle = \Theta(-E_k)\,\delta_{\mathbf{k},\mathbf{k'}} , \tag{14}$$

with $\Theta(x)$ the Heaviside step function, the number equation (2) gives

$$N = N_R + N_G + N_B , \tag{15}$$

where

$$N_R = N_G = \frac{1}{2}\sum_\mathbf{k} v_k^2 \tag{16}$$

and

$$N_B = \sum_\mathbf{k} \Theta\left(\mu - \frac{\hbar^2 k^2}{2m}\right) . \tag{17}$$

Similarly, the gap equation (3) gives

$$-\frac{1}{g} = \frac{1}{V}\sum_\mathbf{k} \frac{1}{2E_k} . \tag{18}$$

The chemical potential μ and the gap energy Δ are obtained by solving equations (15) and (18). In the continuum limit, due to the choice of a contact potential, the gap equation (18)

4

diverges in the ultraviolet. This divergence is linear in three dimensions and logarithmic in two dimensions. We shall face this problem in the next two sections.

Another interesting quantity is the the number of red-green pairs in the lowest state, i.e. the condensate number of red-green pairs, that is given by [29, 30, 32, 33]

$$N_0 = \int d^3\mathbf{r}_1 \, d^3\mathbf{r}_2 \, |\langle \hat{\psi}_G(\mathbf{r}_1)\hat{\psi}_R(\mathbf{r}_2)\rangle|^2 = \sum_{\mathbf{k}} u_k^2 v_k^2 \ . \tag{19}$$

In the last years two experimental groups [26–28] have analyzed the condensate fraction of three-dimansional ultra-cold two-hyperfine-component Fermi vapors of ^{6}Li atoms in the crossover from the Bardeen-Cooper-Schrieffer (BCS) state of Cooper Fermi pairs to the Bose-Einstein condensate (BEC) of molecular dimers. These experiments are in quite good agreement with mean-field theoretical predictions [29, 30] and Monte-Carlo simulations [31] at zero temperature, while at finite temperature beyond-mean-field corrections are needed [32, 33]. Here we show how to calculate the condensate fraction N_0/N for the three-component Fermi gas at zero temperature [25] in three [29] and two [34] dimensions. Finally, we calculate the first sound velocity c_s of the three-component system by using the zero-temperature thermodynamic formula [35]

$$c_s = \sqrt{\frac{n}{m}\frac{d\mu}{dn}} \tag{20}$$

where μ is the chemical potential of the Fermi gas and n the total density. The sound velocity c_s, which is the Nambu-Goldstone mode of pairing breaking of SU(3) symmetry, has been previously analyzed by He, Jin and Zhuang [18] in the three dimensional case. Here we study c_s in the two dimensional case too.

III. THREE DIMENSIONAL CASE

In three dimensions a suitable regularization [21, 23] of the gap equation (18) is obtained by introducing the inter-atomic scattering length a_F via the equation

$$-\frac{1}{g} = -\frac{m}{4\pi\hbar^2 a_F} + \frac{1}{V}\sum_{\mathbf{k}}\frac{m}{\hbar^2 k^2} \ , \tag{21}$$

and then subtracting this equation from the gap equation (18). In this way one obtains the three-dimensional regularized gap equation

$$-\frac{m}{4\pi\hbar^2 a_F} = \frac{1}{V}\sum_{\mathbf{k}}\left(\frac{1}{2E_k} - \frac{m}{\hbar^2 k^2}\right) \ . \tag{22}$$

In the three-dimensional continuum limit $\sum_{\mathbf{k}} \to V/(2\pi)^3 \int d^3\mathbf{k} \to V/(2\pi^2) \int k^2 dk$ from the number equation (15) with (16) and (17) we find the total number density as

$$n = \frac{N}{V} = n_R + n_G + n_B ,\tag{23}$$

with

$$n_R = n_G = \frac{1}{2}\frac{(2m)^{3/2}}{2\pi^2\hbar^3}\Delta^{3/2}\, I_2\Big(\frac{\mu}{\Delta}\Big) ,\tag{24}$$

and

$$n_B = \frac{1}{3}\frac{(2m)^{3/2}}{2\pi^2\hbar^3}\mu^{3/2}\,\Theta(\mu) .\tag{25}$$

The renormalized gap equation (22) becomes instead

$$-\frac{1}{a_F} = \frac{2(2m)^{1/2}}{\pi\hbar}\Delta^{1/2}\, I_1\Big(\frac{\mu}{\Delta}\Big) ,\tag{26}$$

where $k_F = (6\pi N/(3V))^{1/3} = (2\pi^2 n)^{1/3}$ is the Fermi wave number. Here $I_1(x)$ and $I_2(x)$ are the two monotonic functions

$$I_1(x) = \int_0^{+\infty} y^2\left(\frac{1}{\sqrt{(y^2-x)^2+1}} - \frac{1}{y^2}\right) dy ,\tag{27}$$

$$I_2(x) = \int_0^{+\infty} y^2\left(1 - \frac{y^2-x}{\sqrt{(y^2-x)^2+1}}\right) dy ,\tag{28}$$

which can be expressed in terms of elliptic integrals, as shown by Marini, Pistolesi and Strinati [23]. In a similar way we get the condensate density of the red-green pair as

$$n_0 = \frac{N_0}{V} = \frac{m^{3/2}}{8\pi\hbar^3}\Delta^{3/2}\sqrt{\frac{\mu}{\Delta} + \sqrt{1+\frac{\mu^2}{\Delta^2}}} .\tag{29}$$

This equation and the gap equation (26) are the same of the two-component superfluid fermi gas (see [29]) but the number equation (15), with (16) and (17), is clearly different. Note that all the relevant quantities can be expressed in terms of the ratio

$$x_0 = \frac{\mu}{\Delta} ,\tag{30}$$

where $x_0 \in]-\infty,\infty[$. In this way the scaled energy gap Δ/ϵ_F and the scaled chemical potential μ/ϵ_F read

$$\frac{\Delta}{\epsilon_F} = \frac{x_0}{I_2(x_0) + \frac{1}{3}x_0^{3/2}\Theta(x_0)} ,\tag{31}$$

$$\frac{\mu}{\epsilon_F} = \frac{1}{I_2(x_0) + \frac{1}{3}x_0^{3/2}\Theta(x_0)} \ , \tag{32}$$

where $\epsilon_F = \hbar^2 k_F^2/(2m) = (2\pi^2 n)^{2/3}\hbar^2/(2m)$ is the Fermi energy of the 3D ideal three-component Fermi gas with total density n. The fraction of red fermions, which is equal to the fraction of green fermions, is given by

$$\frac{n_R}{n} = \frac{n_G}{n} = \frac{I_2(x_0)}{2I_2(x_0) + \frac{2}{3}x_0^{3/2}\Theta(x_0)} \ , \tag{33}$$

while the fraction of blue fermions reads

$$\frac{n_B}{n} = 1 - \frac{I_2(x_0)}{I_2(x_0) + \frac{1}{3}x_0^{3/2}\Theta(x_0)} \ . \tag{34}$$

The fraction of condensed red-green pairs is instead

$$\frac{n_0}{n} = \frac{\pi}{8\sqrt{2}} \frac{\sqrt{x_0 + \sqrt{1 + x_0^2}}}{I_2(x_0) + \frac{1}{3}x_0^{3/2}\Theta(x_0)} \ . \tag{35}$$

Finally, the adimensional interaction strength of the BCS-BEC crossover is given by

$$y = \frac{1}{k_F a_F} = -\frac{2}{\pi} \frac{I_1(x_0)}{\left(I_2(x_0) + \frac{1}{3}x_0^{3/2}\Theta(x_0)\right)^{1/3}} \ . \tag{36}$$

We can use these parametric formulas of x_0 to plot the density fractions as a function of the scaled interaction strength y.

In the upper panel of Fig. 1 we plot the energy gap Δ (in units of the Fermi energy ϵ_F) as a function of scaled interaction strength $y = 1/(k_F a_F)$. As expected the gap Δ is exponentially small in the BCS region ($y \ll -1$), it becomes of the order of the Fermi energy ϵ_F at unitarity ($y = 0$), and then it inceases in the BEC region ($y \gg 1$). In the lower panel of Fig. 1 we show instead the scaled chemical potential μ/ϵ_F as a function of scaled interaction strength $y = 1/(k_F a_F)$. In the BCS region ($y \ll -1$) the chemical potential μ is positive and practically equal to the Fermi energy ϵ_F of the ideal gas; at unitarity ($y = 0$) the μ is still positive but close to zero; it becomes equal to zero at $y \simeq 0.6$ and then diminishes as $-y^2$ (half the binding energy of the formed dimers).

In the upper panel of Fig. 2 we plot the fraction of red fermions n_R/n (solid line) and the fraction of blue fermions n_B/n (dashed line) as a function of scaled interaction strength $y = 1/(k_F a_F)$. The behavior of n_G/n is not shown because it is exactly the same of n_R/n. The figure shows that in the deep BCS regime ($y \ll -1$) the system has
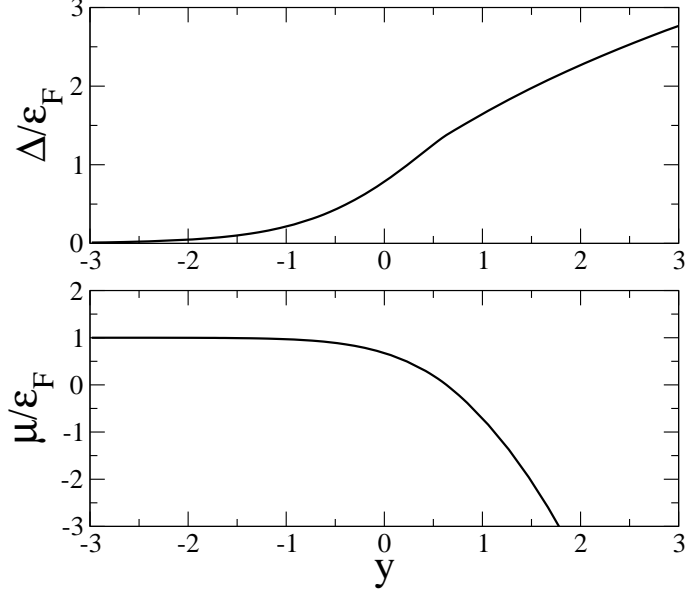
FIG. 1: Ultracold fermions in three-dimensions. Upper panel: scaled energy gap Δ/ϵ_F as a function of scaled interaction strength $y = 1/(k_F a_F)$. Lower panel: scaled chemical potential μ/ϵ_F as a function of scaled interaction strength $y = 1/(k_F a_F)$. Note that $k_F = (2\pi^2 n)^{1/3}$ is the Fermi wave number and $\epsilon_F = \hbar^2 k_F^2/(2m) = (2\pi^2 n)^{2/3}\hbar^2/(2m)$ is the Fermi energy of the 3D ideal three-component Fermi gas with total 3D density n.

$n_R/n = n_G/n = n_B/n = 1/3$. By increasing y the fraction of red and green fermions increases while the fraction of blue fermions decreases. At $y \simeq 0.6$, where $\mu = 0$, the fraction of blue fermions becomes zero, i.e. $n_B/n = 0$ and consequently $n_R/n = n_G/n = 1/2$. For larger values of y there are only the paired red and green particles. This behavior is fully consistent with the findings of Ozawa and Baym [19]. In the lower panel of Fig.1 it is shown the plot of the condensate fraction $n_0/(n/2)$ of red-green pairs through the BCS-BEC crossover as a function of the Fermi-gas parameter $y = 1/(k_F a_F)$. The figure shows that a large condensate fraction builds up in the BCS side already before the unitarity limit ($y = 0$), and that on the BEC side ($y \gg 1$) it rapidly converges to one.

As previously stressed, by using Eq. (20) one can obtain the first sound velocity. In particular, we have found that $\mu = \epsilon_F \, F(y)$, where $F(y)$ is the numerical function plotted in the lower panel of Fig. 1. It is then straightforward to show that

$$c_s = \frac{v_F}{\sqrt{3}}\sqrt{F(y) - \frac{1}{2}yF'(y)} \,. \tag{37}$$

By using this formula we plot in Fig. 3 the scaled sound velocity c_s/v_F as a function of scaled
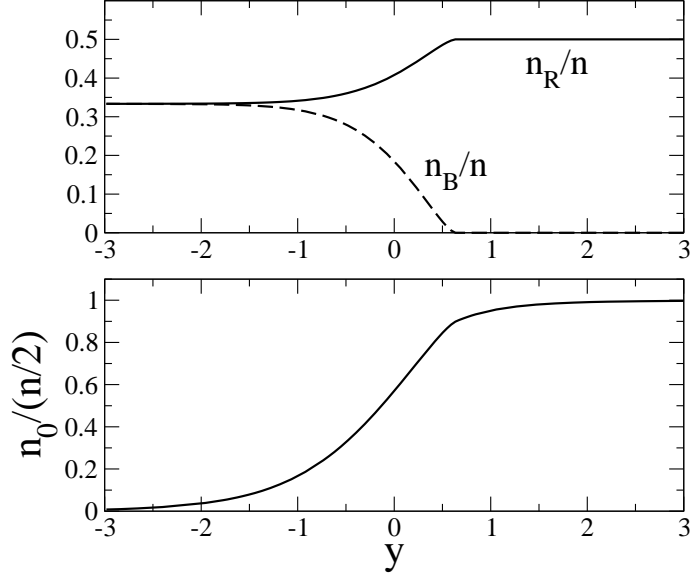
8

FIG. 2: Ultracold fermions in three-dimensions. Upper panel: fraction of red fermions n_R/n (solid line) and fraction of blue fermions n_B/n (dashed line) as a function of scaled interaction strength $y = 1/(k_F a_F)$. Lower panel: condensed fraction of red-green particles n_0/n as a function of scaled interaction strength $y = 1/(k_F a_F)$. Units as in Fig. 1.

interaction strength $y = 1/(k_F a_F)$. The curve shows that c_s/v_F decreases by increasing y and it shows a knee at $y \simeq 0.6$, where the chemical potential changes sign.

IV.   TWO DIMENSIONAL CASE

A two-dimensional Fermi gas can be obtained by imposing a very strong confinement along one of the three spatial directions. In practice, the potential energy E_p of this strong external confinement must be much larger than the total chemical potential μ_{3D} of the fermionic system: $\mu_{3D} \ll 2E_P$ [37]. Contrary to the three-dimensional case, in two dimensions quite generally a bound-state energy ϵ_B exists for any value of the interaction strength g between atoms [22, 23]. For the contact potential the bound-state equation is

$$-\frac{1}{g} = \frac{1}{V} \sum_{\mathbf{k}} \frac{1}{\frac{\hbar^2 k^2}{2m} + \epsilon_B} , \tag{38}$$

9
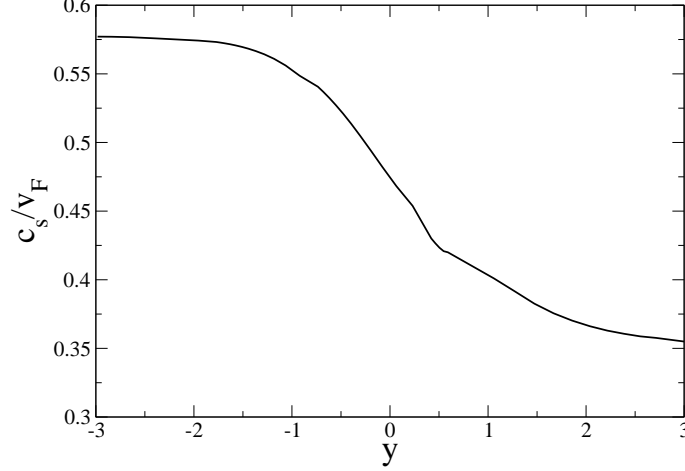
FIG. 3: Ultracold fermions in three-dimensions. Scaled sound velocity c_s/v_F as a function of scaled interaction strength $y = 1/(k_F a_F)$. Units as in Fig. 1, with $v_F = \hbar k_F/m$ the Fermi velocity of the 3D ideal three-component Fermi gas.

and then subtracting this equation from the gap equation (18) one obtains the two-dimensional regularized gap equation [22, 23]

$$\sum_{\mathbf{k}} \left(\frac{1}{\frac{\hbar^2 k^2}{2m} + \epsilon_B} - \frac{1}{2E_k} \right) = 0 \; . \tag{39}$$

Note that, for a 2D inter-atomic potential described by a 2D circularly symmetric well of radius R_0 and depth U_0, the bound-state energy ϵ_B is given by $\epsilon_B \simeq \hbar^2/(2mR_0^2) \exp\left(-2\hbar^2/(mU_0 R_0^2)\right)$ with $U_0 R_0^2 \to 0$ [36].

In the two-dimensional continuum limit $\sum_{\mathbf{k}} \to V/(2\pi)^2 \int d^2\mathbf{k} \to V/(2\pi) \int k dk$, the Eq. (39) gives

$$\epsilon_B = \Delta \left(\sqrt{1 + \frac{\mu^2}{\Delta^2}} - \frac{\mu}{\Delta} \right) \; . \tag{40}$$

Note that here V is the 2D volume of the gas, i.e. an area. Instead, the number equation (15) with (16) and (17) gives the total number density as

$$n = \frac{N}{V} = n_R + n_G + n_B \; , \tag{41}$$

where V is a two-dimensional volume (i.e. an area), the red and green densities are

$$n_R = n_G = \frac{1}{2} \left(\frac{m}{2\pi\hbar^2} \right) \Delta \left(\frac{\mu}{\Delta} + \sqrt{1 + \frac{\mu^2}{\Delta^2}} \right) \; , \tag{42}$$

10

while the blue density reads

$$n_B = \Big(\frac{m}{2\pi\hbar^2}\Big)\mu \, \Theta(\mu) \,. \tag{43}$$

Finally, the condensate density of red-green pairs is given by

$$n_0 = \frac{1}{4}\Big(\frac{m}{2\pi\hbar^2}\Big)\Delta \left(\frac{\pi}{2} + \arctan\big(\frac{\mu}{\Delta}\big)\right) \,. \tag{44}$$

Also in this two-dimensional case all the relevant quantities can be expressed in terms of the ratio $x_0 = \mu/\Delta$, where $x_0 \in]-\infty, \infty[$. In particular, the scaled pairing gap is given by

$$\frac{\Delta}{\epsilon_F} = \frac{3}{x_0 + \sqrt{1+x_0^2} + x_0\Theta(x_0)} \,, \tag{45}$$

while the scaled chemical potential reads

$$\frac{\mu}{\epsilon_F} = \frac{3x_0}{x_0 + \sqrt{1+x_0^2} + x_0\Theta(x_0)} \,, \tag{46}$$

where the two-dimensional Fermi energy $\epsilon_F = \hbar^2 k_F^2/(2m)$ of the 2D ideal three-component Fermi gas with 2D total density n is given by $\epsilon_F = \pi\hbar^2 n/m$ with $k_F = (4\pi n/3)^{1/2}$ the Fermi wave number.

The fraction of red fermions, which is equal to the fraction of green fermions, is given by

$$\frac{n_R}{n} = \frac{n_G}{n} = \frac{x_0 + \sqrt{1+x_0^2}}{2[x_0 + \sqrt{1+x_0^2} + x_0 \, \Theta(x_0)]} \,, \tag{47}$$

the fraction of blue fermions is

$$\frac{n_B}{n} = 1 - 2\frac{n_R}{n} \,, \tag{48}$$

and the condensate fraction is

$$\frac{n_0}{n} = \frac{\frac{\pi}{2} + \arctan(x_0)}{4[x_0 + \sqrt{1+x_0^2} + x_0 \, \Theta(x_0)]} \,. \tag{49}$$

It is convenient to express the bound-state energy ϵ_B in terms of the Fermi energy ϵ_F. In this way we find

$$\frac{\epsilon_B}{\epsilon_F} = 3\frac{\sqrt{1+x_0^2} - x_0}{x_0 + \sqrt{1+x_0^2} + x_0 \, \Theta(x_0)} \,, \tag{50}$$

We can now use these parametric formulas of x_0 to plot the fractions as a function of the scaled bound-state energy ϵ_B/ϵ_F.

In the upper panel of Fig. 4 we plot the scaled energy gap Δ/ϵ_F as a function of scaled binding energy ϵ_B/ϵ_F. The gap Δ is extremely small in the "BCS region" ($\epsilon_B/\epsilon_F \ll 1/2$),
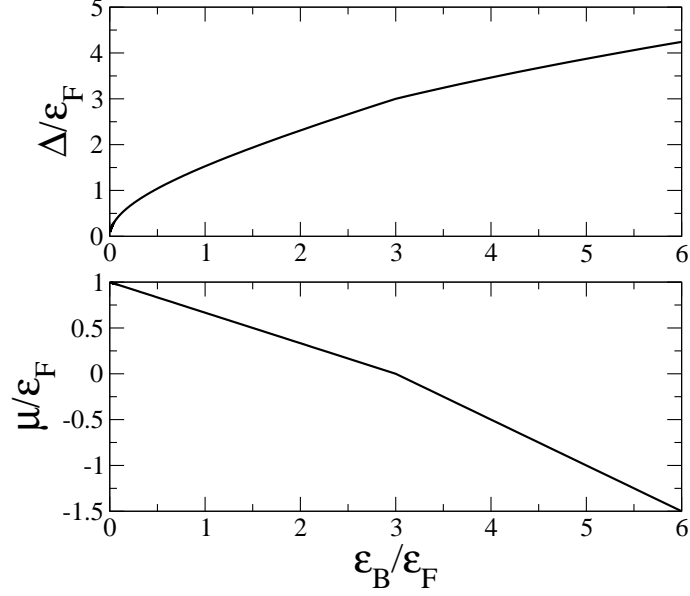
FIG. 4: Ultracold fermions in two-dimensions. Upper panel: scaled energy gap Δ/ϵ_F as a function of scaled bound-state energy ϵ_B/ϵ_F. Lower panel: scaled chemical potential μ/ϵ_F as a function of scaled bound-state energy ϵ_B/ϵ_F. Note that $k_F = (4\pi n/3)^{1/2}$ is the Fermi wave number and $\epsilon_F = \hbar^2 k_F^2/(2m) = (4\pi n/3)\hbar^2/(2m)$ is the Fermi energy of the 2D ideal three-component Fermi gas with total 2D density n.

it becomes of the order of the Fermi energy ϵ_F at $\epsilon_B/\epsilon_F = 1/2$, and then it inceases in the "BEC region" ($\epsilon_B/\epsilon_F \gg 1/2$). In the lower panel of Fig. 4 we show instead the scaled chemical potential μ/ϵ_F as a function of scaled binding energy ϵ_B/ϵ_F. In the BCS region ($\epsilon_B/\epsilon_F \ll 1/2$) the chemical potential μ is positive and decreases as $\mu = \epsilon_F - \epsilon_B/3$; μ becomes equal to zero at $\epsilon_B/\epsilon_F = 3$ and then it further decreases linearly as $\mu = (3\epsilon_F - \epsilon_B)/2$.

In the upper panel of Fig. 5 we plot the fraction of red fermions n_R/n (solid line) and the fraction of blue fermions n_B/n (dashed line) as a function of scaled bound-state energy ϵ_B/ϵ_F. The behavior of n_G/n is not shown because it is exactly the same of n_R/n. The figure shows that in the deep BCS regime ($\epsilon_B/\epsilon_F \ll 1$) the system has $n_R/n = n_G/n = N_B/n = 1/3$. By increasing ϵ_B/ϵ_F the fraction of red and green fermions increases while the fraction of blue fermions decreases. At $\epsilon_B/\epsilon_F = 3$, where $\mu = 0$, the fraction of blue fermions becomes zero. For larger values of ϵ_B/ϵ_F there are only the paired red and green particles. This behavior is quite similar to the one of the three-dimensional case; the main difference is due to the fact that here the curves are linear. In the lower panel of Fig.5 it is shown the condensate
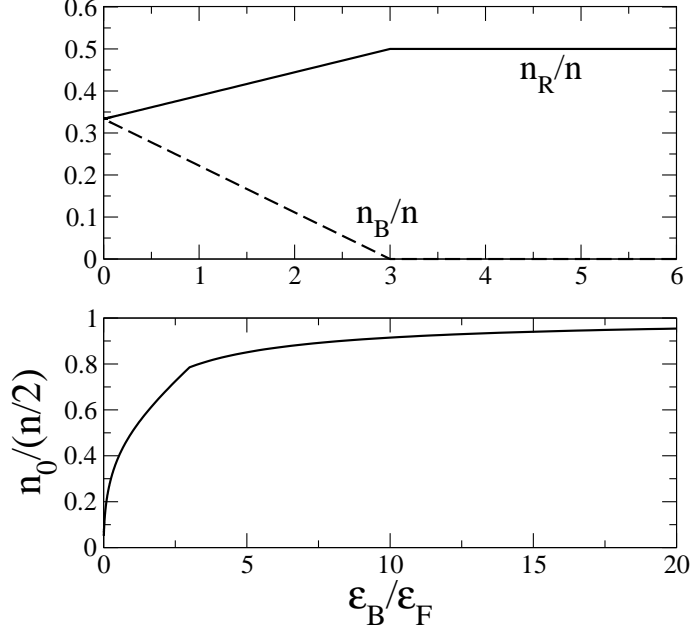
12

FIG. 5: Ultracold fermions in two-dimensions. Upper panel: fraction of red fermions n_R/n (solid line) and fraction of blue fermions n_B/n (dashed line) as a function of scaled bound-state energy ϵ_B/ϵ_F. Lower panel: condensed fraction of red-green particles n_0/n as a function of scaled bound-state energy ϵ_B/ϵ_F. Units as in Fig. 4.

fraction $n_0/(n/2)$ of red-green pairs. In the weakly-bound BCS regime ($\epsilon_B/\epsilon_F \ll 1$) the condensed fraction n_0/n goes to zero, while in the strongly-bound BEC regime ($\epsilon_B/\epsilon_F \gg 1$) the condensed fraction n_0/n goes to $1/2$, i.e. all the red-green Fermi pairs belong to the Bose-Einstein condensate. Notice that the condensate fraction is zero when the bound-state energy ϵ_B is zero. For small values of ϵ_B/ϵ_F the condensed fraction has a very fast grow but then it reaches the asymptotic value $1/2$ very slowly.

Also in 2D, by using Eq. (20) one can obtain the first sound velocity. We have found that $\mu = \epsilon_F \, G(\epsilon_B/\epsilon_F)$, where $G(\epsilon_B/\epsilon_F)$ is the numerical function plotted in the lower panel of Fig. 4. It is then straightforward to show that

$$c_s = \frac{v_F}{\sqrt{2}} \sqrt{G(\frac{\epsilon_B}{\epsilon_F}) - \frac{\epsilon_B}{\epsilon_F} G'(\frac{\epsilon_B}{\epsilon_F})} \; . \tag{51}$$

By using this formula we plot in Fig. 6 the scaled sound velocity c_s/v_F as a function of scaled binding energy ϵ_B/ϵ_F. The curve shows that c_s/v_F is constant, i.e. $c_s/v_F = 1/\sqrt{2}$, by increasing ϵ_B/ϵ_F up to $\epsilon_B/\epsilon_F = 3$ where the chemical potential becomes equal to zero. For a larger value of ϵ_B/ϵ_F the sound velocity c_s jumps to a larger constant value, i.e.
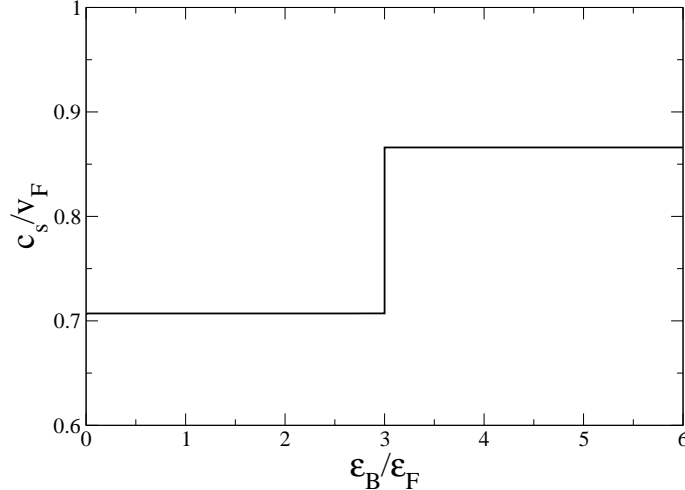
FIG. 6: Ultracold fermions in two-dimensions. Scaled sound velocity c_s/v_F as a function of scaled bound-state energy ϵ_B/ϵ_F. Units as in Fig. 4, with $v_F = \hbar k_F/m$ the Fermi velocity of the 2D ideal three-component Fermi gas.

$c_s/v_F = \sqrt{3}/2$. This kink in the first sound velocity c_s is reminescent of the jumps seen with repulsive fermions with reduced dimensionalities [37, 38] and with dipolar interaction [39].

V. CONCLUSIONS

We have investigated a uniform three-component ultracold fermions by increasing the SU(3) invariant attractive interaction. We have considered the symmetry breaking of the SU(3) symmetry due to the formation of Cooper pairs both in the three-dimensional case and in the two-dimensional one. We have obtained explicit formulas and plots for energy gap, chemical potential, number densities, condensate density, population imbalance and first sound velocity in the full BCS-BEC crossover. In our calculations we have used the zero-temperature mean-field extended BCS theory, which is expected to give reliable results apart in the deep BEC regime [31–33]. Our results are of interest for next future experiments with degenerate gases made of alkali-metal or alkaline-earth atoms. As stressed in the introduction, SU(N) invariant interactions can be experimentaly obtained by using these atomic species [9, 10, 13]. The problem of unequal couplings, and also that of a fixed number of atoms for each component, is clearly of big interest too, and its analysis can be afforded by including more than one order parameter [40].

There are other interesting open problems about superfluid ultracold atoms we want to face in the next future. In particular, we plan to investigate quasi one-dimensional and quasi two-dimensional Bose-Einstein condensates in nonlinear lattices (i.e. with space-dependent interaction strength) [41]. Moreover, we want to analyze the signatures of classical and quantum chaos [42–46] with Bose-Einstein condensates in single-well and double-well configurations, and also in the presence of vortices [47–49]. Finally, we aim to calculate analytically the coupling tunneling energy of bosons by means of the WKB semiclassical quantization [50–53] and comparing it with the numerical results of the Gross-Pitaevskii equation.

[1] A.J. Leggett, Quantum Liquids: Bose Condensation and Cooper Pairing in Condensed-Matter Systems (Oxford Univ. Press, Oxford, 2006).

[2] H.T.C. Stoof, B.M. Dennis, and K. Gubbels, Ultracold Quantum Fields (Springer, Berlin, 2009).

[3] G. Diana, N. Manini, and L. Salasnich, Phys. Rev. A **73** 065601 (2006).

[4] L. Salasnich and N. Manini, Laser Phys. **17**, 169 (2007).

[5] L. Salasnich, F. Ancilotto, and F. Toigo, Laser Phys. Lett. **7**, 78 (2010).

[6] Y. Cheng and S.K. Adhikari, Laser Phys. Lett. **7**, 824 (2010).

[7] Y.I. Yukalov, Laser Phys. Lett. **7**, 467 (2010).

[8] R.F. Shiozaki, G.D. Telles, Y.I. Yukalov, and V.S. Bagnato, Laser Phys. Lett. **8**, 393 (2011).

[9] T.B. Ottenstein, T. Lompe, M. Kohen, A.N. Wenz, and S. Jochim, Phys. Rev. Lett. **101**, 203202 (2008).

[10] J.H. Huckans, J.R. Williams, E.L. Hazlett, R.W. Stites, and K. M. O'Hara, Phys. Rev. Lett. **102**, 165302 (2009).

[11] C. Wu, J.P. Hu, and S.C. Zhang, Phys. Rev. Lett. **91**, 186402 (2003).

[12] C. Wu, Mod. Phys. Lett. B **20**, 1707 (2006).

[13] A.V. Gorshkov, M. Hermele, V. Gurarie, C. Xu, P.S. Julienne, J. Ye, P. Zoller, E. Demler, M.D. Lukin, A.M. Rey, Nature Physics **6**, 289 (2010).

[14] A.G.K. Modawi and A.J. Leggett, J. Low Temp. Phys. **109**, 625 (1997).

[15] C. Honerkamp and W. Hofstetter, Phys. Rev. Lett. **92**, 17040 (2004).

[16] T. Paananen, J.-P. Martikainen, and P. Torma, Phys. Rev. A **73**, 053606 (2006).

[17] C.K. Chung and C.K. Law, Phys. Rev. A **82**, 033620 (2010).

[18] L. He, M Jin, and P. Zhang, Phys. Rev. A **74**, 033604 (2006).

[19] T. Ozawa and G. Baym, Phys. Rev. A **82**, 063615 (2010).

[20] D.M. Eagles, Phys. Rev. **186**, 456 (1969).

[21] A.J. Leggett, in *Modern Trends in the Theory of Condensed Matter*, p. 13, edited by A. Pekalski and J. Przystawa (Springer, Berlin, 1980).

[22] M. Randeria, J.-M. Duan, and L.-Y. Sheih, Phys. Rev. B **41**, 327 (1990).

[23] M. Marini, F. Pistolesi, and G.C. Strinati, Eur. Phys. J. B **1**, 151 (1998).

[24] M.Y. Kagan and S.L. Ogarkov, Laser Phys. **18**, 509 (2008).

[25] L. Salasnich, Phys. Rev. A **83**, 033630 (2011).

[26] M.W. Zwierlein, C.A. Stan, C.H. Schunck, S.M.F. Raupach, A.J. Kerman, and W. Ketterle, Phys. Rev. Lett. **92**, 120403 (2004).

[27] M.W. Zwierlein, C.H. Schunck, C.A. Stan, S.M.F. Raupach, and W. Ketterle, Phys. Rev. Lett. **94**, 180401 (2005).

[28] Y. Inada, M. Horikoshi, S. Nakajima, M. Kuwata-Gonokami, M. Ueda, and T. Makaiyama, Phys. Rev. Lett. **101**, 180406 (2008).

[29] L. Salasnich, N. Manini, and A. Parola, Phys. Rev. A **72**, 023621 (2005).

[30] G. Ortiz and J. Dukelsky, Phys. Rev. A **72**, 043611 (2005).

[31] G. E. Astrakharchik, J. Boronat, J. Casulleras, and S. Giorgini, Phys. Rev. Lett. **95**, 230405 (2005).

[32] Y. Ohashi and A. Griffin, Phys. Rev. A **72**, 063606 (2005).

[33] N. Fukushima, Y. Ohashi, E. Taylor, and A. Griffin, Phys. Rev. A **75**, 033609 (2007).

[34] L. Salasnich, Phys. Rev. A **76**, 015601 (2007).

[35] L.D. Landau and E.M. Lifshits, *Statistical Physics*, Part 2, vol. 9 (Butterworth-Heinemann, Oxford, 1980).

[36] L.D. Landau and E.M. Lifshitz, *Quantum Mechanics. Non Relativistic Theory. Course of Theoretical Physics*, Vol. 3 (Pergamon Press, New York, 1989).

[37] G. Mazzarella, L. Salasnich, and F. Toigo, Phys. Rev. A **79**, 023615 (2009).

[38] L. Salasnich, and F. Toigo, J. Low Temp. Phys. **150**, 643 (2008).

[39] J.P. Kestner and S. Das Sarma, Phys. Rev. A **82**, 033608 (2010).

[40] O.H.T. Nummi, J.J. Kinnunen, and P. Torma, New J. Phys. **13**, 055013 (2011).

[41] Y.V. Kartashov, B.A. Malomed, and L. Torner, Rev. Mod. Phys. **83**, 247 (2011).

[42] L. Salasnich, Phys. Rev. D **52**, 6189 (1995).

[43] L. Salasnich, Mod. Phys. Lett. A **12**, 1473 (1997).

[44] L. Salasnich, Phys. Lett. A **266**, 187 (2000).

[45] A.R. Kolovsky and A. Buchleitner, Europhys. Lett. **68** 632 (2004).

[46] C. Weiss and N. Teichmann, Phys. Rev. Lett. 100, 140408 (2008).

[47] L. Salasnich, Int. J. Mod. Phys. B **14**, 1 (2000).

[48] L. Salasnich, Laser Phys. **14**, 291 (2004).

[49] S.K. Adhikari and L. Salasnich, Phys. Rev. A **75**, 053603 (2007).

[50] M. Robnik and L. Salasnich, J. Phys. A: Math. Gen. **30**, 1711 (1997).

[51] M. Robnik and L. Salasnich, J. Phys. A: Math. Gen. **30**, 1719 (1997).

[52] G. Alvarez, J. Math. Phys. **45**, 3095 (2004).

[53] A.V. Turbiner, Int. J. Mod. Phys. A **25**, 647 (2010).